Journal of Experimental and Applied Physics
Journal Homepage: jeap.ppj.unp.ac.id
Vol. 2, No. 1, March 2024.
ISSN (Print): 2988-0378 ISSN (Online): 2987-9256

Lattice Constants, Structure and Crystal Size of Nanocomposites LiOH/Activated Carbon of Rough Bamboo With Mass Variation

Yulia Febrina[1], Yenni Darvina[1,*], Ratnawulan[1], Fadhila Ulfa Jhora[1]

[1] Department of Physics, Universitas Negeri Padang, Padang 25131, Indonesia

Article History
Received : February, 10th 2024
Revised : February, 25th 2024
Accepted : March, 31st 2024
Published : March 31st 2024

DOI:
https://doi.org/10.24036/jeap.v2i1.44

Corresponding Author
*Author Name: Yenni Darvina
Email: ydarvina@fmipa.unp.ac.id

Abstract: Batteries are reliable electrical energy in the operation of portable electronic devices. Batteries that are often used are lithium batteries. Lithium batteries have the ability to charge quickly, last long and have high energy power but batteries often overheat, affecting the work of the battery. One way to improve the performance of lithium batteries is improve the quality of the anode material. This study aims to determine the lattice constant, structure, and crystal size of carbon, activated carbon, LiOH and variations of LiOH nanocomposite/ rough bamboo activated carbon. This research uses the sol gel method and is characterized using XRD. The mass variations used are 40%: 60%, 50% : 50%, 60% :40%. Carbon has a cubic crystal structure, crystal size of 103 nm. Peak addition occurs on activated carbon because it undergoes an activation process. Activated carbon has a hexagonal crystal structure, smaller crystal size than carbon which 25 nm - 62 nm. LiOH has a tetragonal crystal structure, crystal size 81 nm - 108 nm. The LiOH phase generally has a tetragonal crystal structure, and the carbon phase has a rhombohedral crystal structure. In the 40%: 60% variation has the smallest crystal size of 23 nm - 42 nm, because the addition of activated carbon is more than LiOH so that it affects the crystal size. If the addition of activated carbon is more than LiOH, the crystal size will be smaller.

Keywords: **N**anocomposite; LiOH; Activated Carbon; Rough Bamboo

Journal of Experimental and Applied Physics is an open access article licensed under a Creative Commons Attribution ShareAlike 4.0 International License which permits unrestricted use, distribution, and reproduction in any medium, provided the original work is properly cited. ©2024 by author.

1. Introduction

Batteries are one source of electrical energy that can be relied upon in operating portable electronic devices or can be carried everywhere [1][2][3]. Some electronic devices that use batteries include cell phones, laptops, digital cameras, remote controls, and other electronic equipment [2][4]. One of the batteries that are widely used today is lithium batteries or rechargeable batteries [5][6]. Lithium batteries have fast battery charging capabilities with a

How to cite:
Y. Febrina, Y. Darfina, Ratnawulan and F.U. Jhora, 2024, Lattice Constants, Structure and Crystal Size of Nanocomposites LiOH/Activated Carbon of Rough Bamboo With Mass Variation
Journal of Experimental and Applied Physics, Vol. 2, No.1, page 60-74.

charging time of 2 - 4 hours [7]. Low self-discharge, high energy power, durable if the charging process is appropriate [8], has a relatively long life span and cycle performance that cannot be rivaled by other energy storage devices [9]. In fact, the development of lithium batteries still pays little attention to the characteristics of the batteries used. When in discharge conditions that occur the temperature in the battery will increase [10], causing overheat and has a short life-time so as to affect the work and reduce the life of the battery [9][5].

One of the efforts to improve the performance of the lithium-ion battery is to develop the quality of the electrode material [6]. Lithium ion battery electrodes consist of a positive electrode (cathode) and a negative electrode (anode) [10][11][12]. The working indicators of lithium ion batteries depend on the anode material, which includes energy storage capacity, as well as electrochemical cycling ability [13]. Common materials used as constituents of lithium battery anodes are graphite [14][15]. Graphite has a theoretical capacity of $372\ \mathrm{mAhg^{-1}}$ [10]. This capacity is relatively low so that it is not able to support the increasing capacity needs of electronic devices [16]. In addition, graphite makes the battery cycle short because graphite only operates at potential (>4C) [17]. To overcome the shortcomings of graphite, the active material of the lithium battery anode material must be developed again. One material that can be used is activated carbon material [18]. and the addition of Lithium Hydroxide (LiOH) as a lithium salt that can increase the work of the anode on the capacity of electronic devices [19].

Activated carbon is a material that contains quite a lot of free carbon, has a high absorption capacity [20] and increased pores [21]. Activated carbon has a surface area ranging from 100 to 2000 m/g 2 [22]. Activated carbon has a higher capacity than the theoretical capacity limit of graphite, good cycling stability, and volumetric capacity. $1770\ \mathrm{mAhcm^{-3}}$ [23]. In the manufacture of activated carbon from hazelnut shells [24], producing the optimum specific surface area of carbon which is 391.567 m2/g at 600°C activation temperature. Then the manufacture of activated carbon was developed into a battery anode material [25], resulting in optimal conductivity and capacitance values, which are respectively equal to $1{,}085\ \mathrm{x}\ 10^{-4}$ S/m and $198{,}6\ \mu\mathrm{F}$. Lithium hydroxide (LiOH) can also help improve conductivity because it has an average experimental conductivity of S/m. $129{,}05\ \mathrm{Sm^{-1}}$ [26].

In the synthesis of lithium battery anode material from Lithium Hydroxide (LiOH) and activated carbon from hazelnut shell charcoal [1], producing electrical conductivity and capacitance values, namely $2{,}34\ \mathrm{x}\ 10^{-6}$ S/cm and 327.93 μF. Then developed by comparing the ratio of LiOH / coconut shell activated carbon [16]. The results showed that the active LiOH/coconut shell activated carbon with a ratio of 2: 1 has the highest electrical conductivity with a value of $2{,}064 \times 10^{-3}\ \mathrm{Sm^{-1}}$ [10]. From the above research, it can be concluded that LiOH / activated carbon material can be applied as a nanocomposite forming material.

The material used in the process of making activated carbon in this study is rough bamboo (*Dendrocalamus asper*). Rough bamboo has many benefits, namely as building material, house poles, bridges or walkways and as a tobacco warehouse frame [27][28][29]. In the utilization of rough bamboo, of course, various processing is carried out and a large amount of bamboo waste is produced. Waste from Rough bamboo can be used as an ingredient for making activated carbon. The content of activated carbon is very high with a number that exceeds the Indonesian Industrial Standard (SII), which is 337-379 mg/g [30].

Nanocomposites have a role in energy storage materials or battery applications. Nanocomposites are materials made by incorporating nanoparticles to act as fillers in a matrix and multiphase solid materials where each phase has one, two, and three dimensions less than 100 nm [31]. Nanocomposite materials consist of two or more inorganic/organic molecules in some form of combination with a barrier between them of at least one molecule or characterized by nano-sized [5][31][32]. The size of the material that is made nano is an attraction in itself because it can change the characteristics of the material [33]. The nano-sized particles have a high interaction surface area. The more particles that interact, the stronger the material [34][35].

High Energy Milling (HEM) is a unique technique that uses collision energy between crushing balls and chamber walls that are rotated and driven in a certain way. This technique was chosen because it can reduce materials to the nano order (nano particles) in a relatively short time under atmospheric conditions at room temperature during the milling process [36]. HEM is able to produce smaller particles in a shorter milling time [37]. In the preparation of nanocomposites using the sol-gel method. In the study of nano-sized material synthesis methods, the sol gel method is a simple and easy method in its application. In addition to the sol gel method has the ability to control particle size, and the resulting nanoparticles are high purity and homogeneous [38][39][40].

X-Ray Diffraction (XRD) is the most commonly used material characterization method.This technique is used to identify the crystalline phase in the material by determining the lattice structure parameters and obtaining the crystal size [41][42]. X-Ray diffraction is a characterization that utilizes X-rays with wavelengths of 0.5 to 2.5 Å [43]. The working principle of the XRD tool is that the hot filament induces an electrified cathode. The cathode then produces electrons that are directed to the sample. Electrons move quickly through the sample. The speed of the electrons is affected by the potential difference between the cathode and the sample Samples that are pounded by electrons will produce X-rays with a certain energy. The X rays are captured by the detector to be turned into crystallography [44].

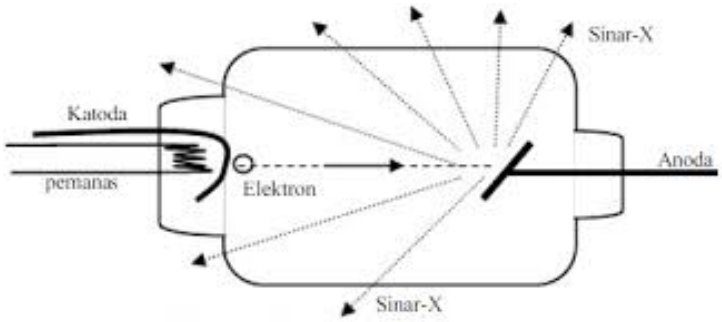

Figure 1. Schematic of an X-ray diffraction apparatus [44]

X-rays have dimensions proportional to the interplanar distance in the crystal. An X-ray beam with a wavelength directed at a crystal surface with an angle of incidence (θ), then the beam will be scattered by the plane of the crystal atoms and produce peaks called diffraction and observed with a diffractor [45]. The method to analyze the crystal structure is the Deybe Scherrer method. The crystalline size is determined based on the broadening of the X-ray diffraction peak that appears. For particles with a nanometer size that contains only one crystallite. Thus, the crystallinity size that can be predicted using the Scherrer method is also the particle size. [41]. The

more crystal fields contained in the sample, the stronger the refraction intensity produced. The peak that appears on the XRD pattern has one crystal plane that has a corresponding orientation on the three-dimensional axis. The peaks obtained from the measurement data were matched with X-ray diffraction standards for all types of materials [46].

This research uses three mass variations, namely 40%: 60%, 50%: 50%, 60%: 40%. This research can determine how the lattice constant, structure, crystal size of carbon and rough bamboo activated carbon, Lithium Hydroxide (LiOH) and mass variation of nanocomposite LiOH /activated carbon of rough bamboo. Furthermore, this research will be applied as a lithium battery anode material.

2. Materials and Method

This type of research is experimental research. This research was conducted with three stages, namely the stage of making activated carbon powder, the stage of making LiOH / activated carbon nanocomposites and the sample characterization stage. At the sample characterization stage, XRD was used to determine the lattice constant, structure, and crystal size of carbon and rough bamboo activated carbon. Lithium Hydroxide (LiOH) and mass variation of LiOH nanocomposite/ rough bamboo activated carbon. Where the mass variations used in this research are 40%: 60%, 50%: 50%, 60%: 40%.

This research was conducted from June to October 2023. The manufacture of carbon, activated carbon and LiOH nanocomposite/ rough bamboo activated carbon was carried out at LLDIKTI Region X Padang. Characterization using (XRD) was carried out at the Material Physics and Biophysics Laboratory of Padang State University. The independent variable in this study is the variation of LiOH/active carbon nanocomposites with a mass ratio of 40% : 60%, 50% : 50%, 60% : 40%. The structure, lattice constant and crystal size of the LiOH/active carbon nanocomposite are the dependent variables of this study. The control variables are H3PO4 and its activation time in making activated carbon, mass concentration of LiOH/activated carbon nanocomposite, temperature and stirring time of nanocomposite, temperature and calcination time of nanocomposite.

The materials used in this study are rough bamboo, H3PO4 20%, LiOH 98%, Polyethylene glycol (PEG) 6000, Sodium chloride (NaCl) 3 M, Citric acid (C6H8O7) 4M, Ethanol (C2H6O) 95%, Aquades. Various equipment used in this study include Furnace, High Energy Miliing (HEM), Standard Test Sieve 120 and 200, porcelain cup, digital scales, measuring cup, spatula, Hot plate magnetic stirrer, oven, pellet mold, hydraulic press, Ph meter and XRD.

The process of making activated carbon powder is carried out through two stages, namely the carbonization and activation stages [26][47]. In the activation process will use a chemical activation process, because it has the advantage that the temperature used is lower than physical activation and also affects the increase in the number of pores of activated carbon [48][49]. The manufacture of activated carbon is based on research [26]. In the carbonization stage, the rough bamboo is cleaned and then dried under the sun until it is dry and has a moisture content of <10%. Then rough bamboo is heated in a furnace with a temperature of 600°C for 60 minutes until it turns into charcoal. Rough bamboo charcoal was pulverized using a mortar and pestle until it was in powder form and then sieved with a 120 mesh sieve, then the charcoal was soaked in 20% H3PO4 for 24 hours. After activation, the charcoal was filtered and rinsed with distilled

water until it reached a neutral pH, then heated using an oven at 900°C for 15 minutes. The activated carbon was pulverized using HEM to produce nano size.

(a) **(b)** **(c)**

Figure 2. (a) Rough bamboo that will be in the furnace. (b) Rough bamboo after the furnace. (c) Screening process

The manufacture of LiOH/activated carbon nanocomposites was carried out based on research [16]. Where the mass variation of LiOH/active carbon nanocomposite is 40%: 60%, 50% : 50%, 60% : 40% with a total amount of LiOH/active carbon nanocomposite of 3g. Then as much as 45 g of PEG 6000 was dissolved with 60 ml of 95% ethanol in a glass with a temperature of 50°C and stirred using a Hot Plate Magnetic Stirrer until homogeneous. Next, mix the LiOH powder / activated carbon into a measuring cup containing a solution of PEG 6000 while stirring 4 molar citric acid is added until Ph 4-5 (acid), the stirring temperature is increased to 100°C for 1 hour until the solution is gel-shaped. The gel was then put into a petri dish and calcined using a hot plate with a temperature of 300°C. The dried gel was mashed using a mortal and pestle and ready to be sampled and characterized.

Figure 3. Nanocomposite manufacturing process

Then, the samples were characterized using XRD. XRD aims to obtain lattice constant, structure and crystal size. The crystal size can be calculated using the Scherrer equation, the determination refers to the main peaks of the diffractogram pattern [50][51].

$$D = \frac{K\lambda}{\beta \cos\theta} \qquad (1)$$

With D is the crystal grain size, is the X-ray wavelength (Å), is the width of the peak at half maximum (Full Width Half Maximum, FWHM), θ is the Bragg angle. Because XRD uses Cu Kα rays, the wavelength used is 1.54098 Å, and k = 1 [50].

3. Results and Discussion

The synthesis of nanocomposite LiOH/activated carbon of rough bamboo using mass variation of 40%: 60%, 50%: 50%, 60%: 40%, using the sol-gel method. The characterization tool uses XRD which aims to determine the lattice constant, structure, and crystal size of carbon and activated carbon of rough bamboo, LiOH, and mass variations of nanocomposites LiOH/activated carbon of rough bamboo.

The results of the XRD test are in the form of a diffractogram graph using a 2θ angle between 0 - 200°. The diffractogram graph of rough bamboo carbon, activated carbon of rough bamboo and Lithium Hydroxide (LiOH) can be seen from the picture below.

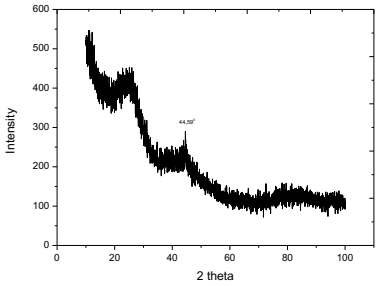

Figure 4. Diffractogram of rough bamboo carbon

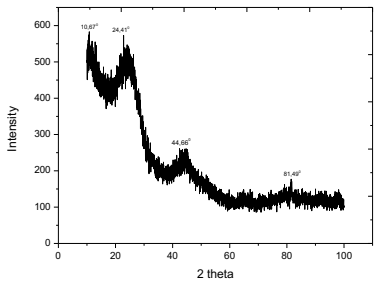

Figure 5. Difractogram graph of activated carbon of rough bamboo

Based on Figures 4 and 5, the relationship between intensity (a.u) and diffraction angle (2θ) and there are several significant intensity peaks at certain angles. Diffraction pattern measurement data of carbon and activated carbon of rough bamboo obtained using the *High Score Plus* application can be seen in the table below.

Table 1. Data of each intensity peak, lattice constant, crystal structure of carbon rough bamboo

The post [°2Th.]	FWHM	Miller index			Intensity (a.u)	Crystal Structure
		h	k	l		
44,59	0,3744	1	0	1	100	Hexagonal

Table 2. Data of each intensity peak, lattice constant, crystal structure of activated carbon of rough bamboo

The post [°2Th.]	FWHM	Miller index			Intensity (a.u)	Crystal Structure
		h	k	l		
10,67	0,6140	0	0	2	55,35	Cubic
44,66	0,2558	1	0	0	100	Hexagonal
81,49	0,4093	0	0	1	49,13	Cubic

Based on table 1, the carbon material has a peak at a diffraction angle of 44.59° with a miller index (101). The lattice constant value at this diffraction angle is the value of a(Å) = 2,27 b(Å) = 2,47 c(Å) = 6,8 with angles $\alpha = 90°$ $\beta = 90°$ and $\gamma = 120°$ resulting in a crystal structure that is

cubic. Furthermore, in activated carbon there are diffraction peaks at angles of 10.67°, 44.66° and 81.49° with miller indices (002), (100), and (001). The value of the lattice constant at this diffraction angle is the value of a(Å) = 2,27 b(Å) = 2,47 c(Å) = 6,8 with angles α = 90° β = 90° and ɣ = 120° resulting in a crystal structure that is cubic and the value of a(Å) = 2,46 b(Å) = 2,46 c(Å) = 6,73 with angles α = 90° β = 90° and ɣ = 120° resulting in a crystal structure that is hexagonal [52]. The addition of diffraction peaks is seen when the carbon after activation becomes activated carbon. By using equation 1, it can determine the crystal size of carbon and activated carbon of rough bamboo contained in the table below.

Table 3. Crystal size values of rough bamboo carbon

K	λ *(nm)*	β *(rad)*	θ (°)	D *(nm)*
0,94	0,154	0,001341	0,07675	103.4656

Table 4. Crystal size values activated carbon of rough bamboo

K	λ (nm)	β (rad)	θ (°)	D (nm)
0,94	0,154	0.005358	0.307008	25.86603
0,94	0,154	0.002233	0.12792	62.07923
0,94	0,154	0,003572	0.204672	38.79936

Based on Table 4 and Table 5, it can be seen that the crystal size of carbon is larger than the crystal size of activated carbon. The crystal size of carbon has a value of 103 nm. While the crystal size of activated carbon has a value of 25 nm - 62 nm. It can be concluded that activated carbon is nano-sized with a crystal size value below 100 nm and can be used as a nanocomposite forming material. Furthermore, the XRD results of the *Lithium Hydroxide* (LiOH) material using the 2θ angle. There is a graph below.

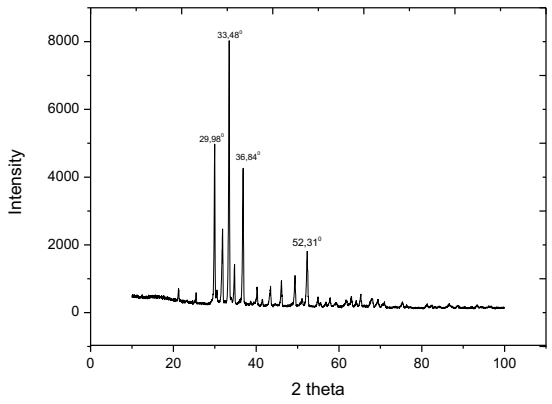

Figure 6. LiOH difractogram graph

Based on Figure 6, states the relationship between intensity (a.u) with diffraction angle (2θ) and there are several significant intensity peaks at certain angles. Diffraction pattern measurement data of carbon and activated carbon of rough bamboo obtained using the High Score Plus application can be seen in the table below.

Table 5. Data of each intensity peak, lattice constant, crystal structure of LiOH

The post [°2Th.]	FWHM	Miller index			Intensity (a.u)	Crystal Structure
		h	k	l		
29,98	0,1790	1	0	1	60,39	Tetragonal
33,48	0,2046	1	1	0	100	Monoclinic
36,84	0,2046	1	0	2	53,18	Tetragonal
52,31	0,1790	2	0	0	21,37	Tetragonal

Based on table 5, LiOH has an optimum peak at a diffraction angle of 33,48°. The millier index at each diffraction angle is (101), (110), (102), (200). The LiOH phase has a lattice constant value of a(Å) = 3,54 b(Å) = 3,54 c(Å) = 4,33 with angles $\alpha = 90°$ $\beta = 90°$ and $\gamma = 90°$ with the crystal structure formed is tetragonal. By using equation 1, it can determine the crystal size of carbon and activated carbon of rough bamboo contained in the table below.

Table 6. LiOH crystal size values

K	λ (nm)	β (rad)	θ (°)	D (nm)
0,94	0,154	0.001562	14.99105	91.85342
0,94	0,154	0.001338	17.37953	108.4756
0,94	0,154	0,001785	18.42281	81.83213
0,94	0,154	0,001562	26,15964	98.85243

Based on table 6, it can be seen that the crystal size of LiOH ranges from 81 nm - 108 nm. At each diffraction angle, the LiOH crystal size is generally nano-sized and can be used as a nanocomposite forming material. The results of XRD characterization using mass variations of nanocomposites LiOH/activated carbon of rough bamboo with variations of 40%: 60%, 50% : 50%, 60% : 40% can be seen in the diffractogram graph below.

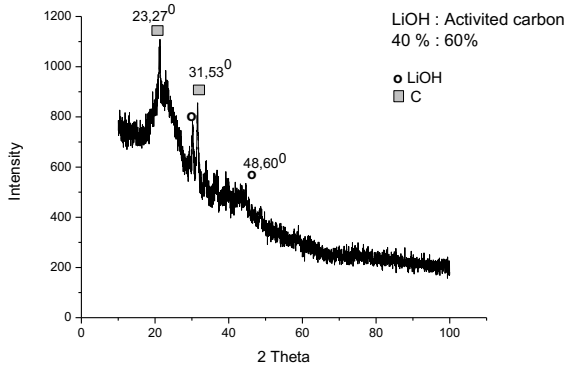

Figure 7. Diffractogram graph of nanocomposite LiOH/ activated carbon of rough bamboo 40% : 60%

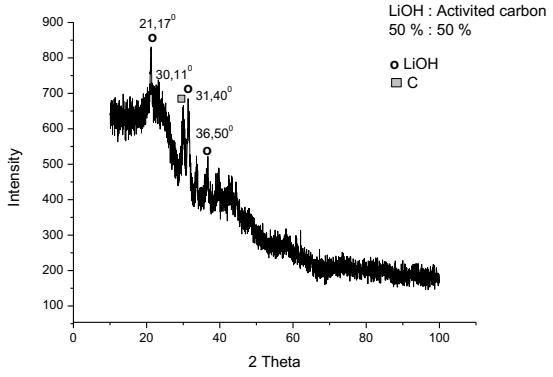

Figure 8. Diffractogram graph of nanocomposite LiOH/ activated carbon of rough bamboo 50% : 50%

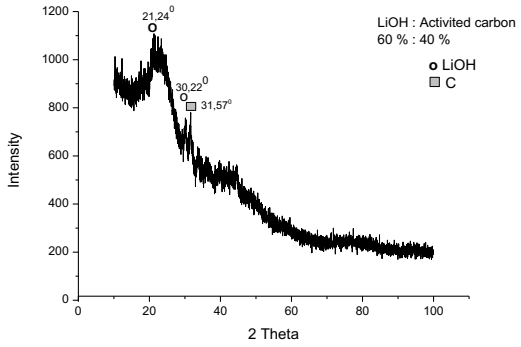

Figure 9. Diffractogram graph of nanocomposite LiOH/ activated carbon of rough bamboo 60% : 40%

Based on Figures 7, 8 and 9, the relationship between intensity (a.u) and diffraction angle (2θ) and there are several significant intensity peaks at certain angles. Diffraction pattern measurement data of carbon and Rough bamboo activated carbon obtained using the High Score Plus application can be seen in the table below.

Table 7. Data of each intensity peak, lattice constant, crystal structure of the nanocomposite LiOH/ activated carbon of rough bamboo 40% : 60%

The post [°2Th.]	FWHM	Miller index			Intensity (a.u)	Crystal Structure
		h	k	l		
23,27	0,6140	1	0	1	33,51	Monoclinic
30,20	0,4093	1	1	0	59,01	Tetragonal
31,53	0,2258	0	0	18	100	Rhombohedral
48,60	0,6140	0	0	14	13,85	Rhombohedral

Table 8. Data of each intensity peak, lattice constant, crystal structure of the nanocomposite LiOH/ activated carbon of rough bamboo 50% : 50%

The post [°2Th.]	FWHM	Miller index			Intensity (a.u)	Crystal Structure
		h	k	l		
21,17	0,3070	0	0	1	63,73	Tetragonal
30,11	0,4093	0	0	18	76,67	Rhombohedral
31,40	0,6140	1	0	1	100	Tetragonal
36,50	0,8186	1	0	2	31,54	Tetragonal

Table 9. Data of each intensity peak, lattice constant, crystal structure of the nanocomposite LiOH/ activated carbon of rough bamboo 60% : 40%

The post [°2Th.]	FWHM	Miller index			Intensity (a.u)	Crystal Structure
		h	k	l		
21,34	0,6140	0	0	1	55,73	Monoclinic
30,22	0,5116	0	0	18	78,52	Tetragonal
31,57	0,3070	1	0	1	100	Rhombohedral

Based on tables 7, 8 and 9, in each variation of the LiOH nanocomposite/rough bamboo activated carbon produces an optimum peak at a diffraction angle of 31°. Generally, the LiOH phase in each variation has a miller index of (110), (101), and (0018), respectively. The value of the kisi constant is the value of a(Å) = 3,54 b (Å) = 3,54 c (Å) = 4,33 with angles $\alpha = 90°$ $\beta = 90°$ and $\gamma = 90°$ with the crystal structure formed is tetragonal. For the carbon phase, the miller indices are (0014), (0018), and (101), respectively. The value of the kition constant is the value of a(Å) = 2,46 b(Å) = 2,46 c(Å) = 5,33 with angles $\alpha = 90°$ $\beta = 90°$ and $\gamma = 120°$ with the crystal structure formed is rhombohedral. By using equation 1, it can determine the crystal size of carbon and activated carbon of rough bamboo contained in the table below.

Table 10**.** Crystal size values of nanocomposites LiOH/activated carbon using a variation of 40%: 60%

K	λ (nm)	β (rad)	θ (°)	D (nm)
0,94	0,154	0,003570	0,003088	42,258214
0,94	0,154	0,005355	0,004570	29,944394
0,94	0,154	0,007140	0,005740	23,370558
0,94	0,154	0,005355	0,003541	39,138715

Table 11. Crystal size values of nanocomposites LiOH/activated carbon using a variation of 50%: 50%

K	λ (nm)	β (rad)	θ (°)	D (nm)
0,94	0,154	0,002677	0,002497	55,506459
0,94	0,154	0,003570	0,003088	44,874757
0,94	0,154	0,005355	0,004570	30,322659
0,94	0,154	0,007140	0,005740	24,145776

Table 12. Crystal size values of nanocomposites LiOH/activated carbon using a variation of 60%: 40%

k	λ (nm)	β (rad)	θ (°)	D (nm)
0,94	0,154	0,005355	0,004988	27,787177
0,94	0,154	0,004462	0,003856	35,941048
0,94	0,154	0,002677	0,002281	60,751382

Based on tables 10, 11 and 12, it can be seen that the crystal size in the variation of LiOH nanocomposite / activated carbon rough bamboo 40%: 60% has the smallest crystal size of 23 nm - 42 nm. In the 50% : 50% variation has a crystal size of 24 nm - 55 nm. While in the variation of nanocomposite LiOH/activated carbon of rough bamboo 60%: 40% has the largest crystal size of 27 nm - 60 nm. This shows that if the addition of more activated carbon, the crystal size will be smaller and better where the crystal size on activated carbon is 25 nm - 62 nm can be seen in table 4. If the addition of LiOH more then the size of the crystals will be greater this is due to the size of the crystals in LiOH is 81 nm - 108 nm contained in table 6, then the addition of LiOH more the size of the crystals will be greater. Based on previous research [1], it is explained that the crystal size of the anode material increases with increasing LiOH concentration in the range of 0.2 g - 1.5 g. The smaller the crystal size, the more nano the nanocomposite material. In the results of this study, it can be concluded that the mass variation of nanocomposite LiOH /activated carbon of rough bamboo with 40% : 60% has a small, good crystal size and both of these studies are in accordance with previous research. The addition of more activated carbon has an optimum diffraction angle of 31.53 ° where the value of the lattice constant is the value of a (Å) = 2.46, b (Å) = 2.46, c (Å) = 5.33 with angles $\alpha = 90$ °, $\beta = 90$ ° and $\gamma = 120$ with the crystal structure formed is rhombohedral in the carbon phase. LiOH nanocomposite material/activated carbon of rough bambo after being characterized using XRD has met the standard of being nano particles, which has a crystal size below 100 nm. From the three mass variations of the nanocomposite it can be concluded that the mass variation of 40% 60%, 50%: 50%, 60% : 40% can be used as a material in battery anodes to improve the quality of the anode material and can be tested for electrical properties of the material.

4. Conclusion

The result of XRD characterization is to determine the lattice constant, crystal structure and crystal size of carbon, activated carbon, LiOH and nanocomposite mass variation. The lattice constant of the diffraction angle can determine the crystal structure. Carbon, activated carbon and LiOH are the forming materials of nanocomposite. Carbon has a cubic crystal structure with a crystal size of 103 nm. peak addition occurs on activated carbon because it has undergone an activation process. Activated carbon has a hexagonal crystal structure with a smaller crystal size than carbon, which is 25 nm - 62 nm. *Lithium Hydroxide* (LiOH) has a tetragonal crystal structure with a crystal size of 81 nm - 108 nm. In each nanocomposite variation has LiOH phase and carbon phase. The LiOH phase generally has a tetragonal crystal structure, and the carbon phase has a rhombohedral crystal structure. In the 40% variation: 60% variation has the smallest crystal size of 23 nm - 42 nm, this happens because in this variation the addition of activated carbon is more than LiOH so that it affects the crystal size. In the 60% : 40% variation has the largest crystal size of 27 nm - 60 nm, this happens because the addition of LiOH is more than activated carbon. If the addition of activated carbon is more, the crystal size is smaller and if the addition of LiOH is more, the crystal size is larger. The smaller the crystal size of a material, the more nano the material will be. So the results of the LiOH/activated carbon nanocomposite synthesis can be used as a battery anode material and can be tested for the electrical properties of each mass variation of the nanocomposite.

Acknowledgments

Thanks to the help of various parties, this research can be carried out well. With this, the researcher would like to thank the supervisor, parents, and friends who have helped in completing this research.

References

[1] H. Susana and Astuti, "Effect of LiOH Concentration on Electrical Properties of Lithium Battery Anode Based on Candlenut Shell Activated Carbon," *J. Fis. Unand*, vol. 5, no. 2, pp. 136-141, 2016.

[2] M. T. Afif, I. Ayu, and P. Pratiwi, "Comparison Analysis Of Lithium-Ion, Lithium-Polymer, Lead Acid And Nickel-Metal Hydride Batteries In Electric Car Use - Review," vol. 6, no. 2, pp. 95-99, 2015.

[3] M. Nasution, "Battery Characteristics as Specific Electrical Energy Storage," *JET (Journal Electr.Technol.*,vol.6,no.1,pp.35-40,2021

[4] F. A. Perdana, "Lithium battery," *INKUIRI J. Educ. Science*, vol. 9, no. 2, p. 113, 2021, doi: 10.20961/inkuiri.v9i2.50082.

[5] Rahmi, Ramli, and Y. Darvina, "Analysis Of Electrical Features Of Fe3o4/Pvdf Nanocomposite Synthesized By Sol Gel Method For Lithium Ion Battery Electroda Application," *Pillar Phys.*, vol. 11, no. 2, pp. 73-80, 2018.

[6] A. M. N. Putra and G. Ramadhan, "Li-Ion battery charging with Constant Current, Constant Voltage, Constant Current-Constant Voltage method," *Encyclopedia J.*, vol. 6, no. 1, pp. 546-551, 2023, [Online]. Available: http://jurnal.ensiklopediaku.org

[7] D. Fatahilah, "Effect Of Zirkonium Doping Variations On Lithium Sodium Titanium Oxide (Na2 Li2Ti6-x ZrxO14) on its performance as an active material for lithium ion battery

anodes," 2018.
[8] J. Lu, Z. Chen, F. Pan, Y. Cui, and K. Amine, "High-Performance Anode Materials for Rechargeable Lithium-Ion Batteries," *Electrochem. Energy Rev.*, no. 0123456789, 2018, doi: 10.1007/s41918-018-0001-4.
[9] T. P. Cahyono, T. Hardianto, and B. S. Kaloko, "Testing the Characteristics of Lithium-Ion Batteries with Fuzzy Methods with Varying Loads," *J. Current Electro Indones.*, vol. 6, no. 3, p. 82, 2020, doi: 10.19184/jaei.v6i3.19708.
[10] S. Han, D. Jung, J. Jeong, and E. Oh, "Effect of pyrolysis temperature on carbon obtained from green tea biomass for superior lithium ion battery anodes," *Chem. Eng. J.*, vol. 254, pp. 597-604, 2014, doi: 10.1016/j.cej.2014.06.021.
[11] B. Nicholas, D. Bresser, and S. Passerini, "Secondary Lithium-Ion Battery Anodes: From First Commercial Batteries to Recent Research Activities Addressing the challenges in rechargeable lithium-ion battery technologies," no. 1, pp. 34-44, 2015.
[12] P. Taylor, X. Zeng, J. Li, and N. Singh, "Critical Reviews in Environmental Science and Technology Recycling of Spent Lithium-Ion Battery: A Critical Review," no. October 2014, pp. 37-41, 2013, doi: 10.1080/10643389.2013.763578.
[13] A. Aflahannisa and A. Astuti, "Synthesis of Carbon-TiO2 Nanocomposite as Lithium Battery Anode," *J. Fis. Unand*, vol. 5, no. 4, pp. 357-363, 2016, doi: 10.25077/jfu.5.4.357-363.2016.
[14] J. Ni, Y. Huang, and L. Gao, "A high-performance hard carbon for Li-ion batteries and supercapacitors application," *J. Power Sources*, vol. 223, pp. 306-311, 2013, doi: 10.1016/j.jpowsour.2012.09.047.
[15] A. F. Nofitasari, "Co 3 O 4 as Anode Material in Li-ion Batteries: Thermal and Morphological Analysis," no. June, pp. 1-12, 2017.
[16] A. Syifaurrahma, Amelli, and Y. Astuti, "Effects of LiOH/Coconut Shell Activated Carbon Ratio on Conductivity of Lithium Ion Battery Anode Active Material," 2021.
[17] C. Zhao, L. Liu, Q. Zhang, J. Rogers, H. Zhao, and Y. Li, "Synthesis of Carbon-TiO2 nanocomposites with enhanced reversible capacity and cyclic performance as anodes for lithium-ion batteries," *Electrochim. Acta*, vol. 155, pp. 288-296, 2015, doi: 10.1016/j.electacta.2014.12.167.
[18] V. Yudha, Y. Afza, M. Muldarisnur, and Y. Yetri, "Analysis of the Effect of NaCl Electrolyte Concentration on the Characteristics of Activated Carbon from Cocoa Fruit Peel," vol. 10, no. 4, pp. 486-492, 2021.
[19] X. L. Yao *et al.*, "Comparative study of trimethyl phosphite and trimethyl phosphate as electrolyte additives in lithium ion batteries," *J. Power Sources*, vol. 144, no. 1, pp. 170-175, 2005, doi: 10.1016/j.jpowsour.2004.11.042.
[20] I. F. Fanani, N and Ulfindrayani, "Bamboo Waste Using Acid Activator," *Synthesis and Characterization of Activated Carbon from Bamboo Waste Using Pospic Acid*, pp. 741-746, 2019.
[21] Darmayanti and N. Rahman, "Adsorption Of Timbal (Pb) And Zink (Zn) From Their Solution By Using Biocharcoal Of Chicken Leather Kepok Based On Ph Variations Adsorption of Plumbum (Pb) and Zinc (Zn) From Its Solution by Using Biological Charcoal (Biocharcoal) of Ke," vol. 1, no. November, pp. 159-165, 2012.
[22] D. Indarto, "Utilization of Banana Peel Waste as Activated Carbon," *User Influence. YELLOW TURKEY (Cucurbita Moschata) Pasta For Substitution Of Thicky Turkey With Addition Of Angkak Turkey In The Making Of Dry Mie,* vol. 15, no. 1, pp. 165-175, 2019.
[23] T. Kim, C. Jo, W. Lim, J. Lee, J. Lee, and K. Lee, "Facile conversion of activated carbon to battery anode material using microwave graphitization," *Carbon N. Y.*, vol. 104, pp. 106-111, 2016, doi: 10.1016/j.carbon.2016.03.021.
[24] A. M. Taspika, "Preparation of Porous Carbon Capacitor Electrode from Candlenut Shell

(Aleurites Moluccana) as Capacitive Deionization System," *J. Fis. Unand*, vol. 4, no. 2, pp. 173-177, 2015.
[25] V. S. I. Negara and Astuti, *Effect of Sintering Temperature of Candlenut Shell Based Activated Carbon on Electrical Properties of Lithium Battery Anode,* vol. 4, no. 2. 2015.
[26] M. Manurung, E. Sahara, and S. Sihombing, "Preparation and Characterization of Activated Charcoal from Bamboo Apus with H3PO4 Activator," 2019.
[27] S. Ramadhan, "Test of Adsorption Rate of Rough Bamboo Stem Activated Carbon as Filter Media in Produced Water Treatment Process," 2002.
[28] Subyakto, E. Hermiati, D. H. Y. Yanto, and Fitria, "Manufacturing Process of Nano-sized Cellulose Fiber from Sisal and Bamboo Rough." 2009.
[29] E. T. Bahtiar, A. P. Imanullah, D. Hermawan, N. Nugroho, and Abdurachman, "Structural grading of three sympodial bamboo culms (Hitam, Andong, and Tali) subjected to axial compressive load," *Eng. Struct.*, vol. 181, no. December 2017, pp. 233-245, 2019, doi: 10.1016/j.engstruct.2018.12.026.
[30] E. M. Hutapea, Iwantono, R. Farma, Saktioto, and Awitdrus, "Preparation and Characterization of Activated Carbon from Bamboo Rough (Dendrocalamus Asper) with Microwave-Assisted KOH Activation," *J. Komun. Fis. Indones.*, vol. 14, no. 02, pp. 1-6, 2017.
[31] R. Ahdiaty, "Anion Adsorption In Aqueous Solution With Magnetic Nanocomposite Fe3o4/Activated Carbon Thesis Rahmi Ahdiaty Nim: 19923019 Chemistry Master Study Program Chemistry Department Faculty Of Mathematics," 2022.
[32] Y. Dhamayanti *et al.*, "Photodegradation of Methylene Blue, and Rhodamine B, with Al2o3, Tio2, and H2o2 Photocatalysts Determined by Visible Light Spectrophotometry," *Pros. Semin. Nas. Kim.*, vol. 11, no. 9, pp. 1689-1699, 2015.
[33] A. P. Swardhani, F. Iskandar, M. Abdullah, and Khairurrijal, "Initial Study of Fe2O3/C Nanocomposite Synthesis by Microwave Heating and Calcination Method," pp. 61-64, 2013.
[34] B. W. Nuryadin and K. Khairurrijal, "Fabrication of Super Strong, Lightweight and Transparent Nanocomposite Materials Using Simple Mixing Method," no. January, 2008.
[35] Y. Suyono, "Initial study of nanocomposite manufacturing with," pp. 63-69, 2012.
[36] P. Guay, B. L. Stansfield, and A. Rochefort, "On the control of carbon nanostructures for hydrogen storage applications," vol. 42, pp. 2187-2193, 2004, doi: 10.1016
[37] A. F. Ramdja, M. Halim, and J. Handi, "Preparation of Activated Carbon from Banana Fronds (Cocus nucifera)," vol. 15, no. 0258, pp. 1-8, 2008.
[38] Y. M. Liza, R. C. Yasin, S. S. Maidani, and R. Zainul, "Gel Sol: Principle and Technique," *Ina. Pap.*, pp. 1-19, 2018.
[39] A. Ardiansyah and S. Wahyuni, "Synthesis of Nanosilica with Sol-Gel Method and Hydrophobicity Test on Acrylic Paint," *Indonesia. J. Chem. Sci.*, vol. 4, no. 3, pp. 83-90, 2015.
[40] G. Budiharti and Z. A. I. Supardi, "Synthesis of Silica Nanoparticles Using the Sol-Gel Method," *J. Inov. Fis. Indones.*, vol. 4, no. 3, pp. 22-25, 2015.
[41] B. Ingham, T. H. Lim, C. J. Dotzler, A. Henning, M. F. Toney, and R. D. Tilley, "How nanoparticles coalesce: An in situ study of Au nanoparticle aggregation and grain growth," *Chem. Mater.*, vol. 23, no. 14, pp. 3312-3317, 2011, doi: 10.1021/cm200354d.
[42] I. L. Putama Mursal, "Characterization of Xrd and Sem on Nanoparticle Materials and the Role of Nanoparticle Materials in Drug Delivery System," *Pharma Xplore J. Ilm. Pharm.*, vol. 3, no. 2, pp. 214-221, 2018, doi: 10.36805/farmasi.v3i2.491.
[43] R. Sharma, D. P. Bisen, U. Shukla, and B. G. Sharma, "X-ray diffraction: a powerful method of characterizing nanomaterials," *Recent Res. Sci. Technol.*, vol. 4, no. 8, pp. 77-79, 2012, [Online]. Available: http://recent-science.com/
[44] A. Chagnes and B. Pospiech, "A brief review on hydrometallurgical technologies for recycling spent lithium-ion batteries," no. April, 2013, doi: 10.1002/jctb.4053.

[45] L. M. Khaskhanova *et al.*, "Scanning Electron Microscopy," *J. Int. Dent. Med. Res.*, vol. 15, no. 1, pp. 107-110, 2022, doi: 10.21273/hortsci.9.5.414.
[46] P. Salame, V. Pawade, and B. A. Bhanvase, *Characterization Tools and Techniques for Nanomaterials*, no. January. 2018. doi: 10.1016/B978-0-12-813731-4.00003-5.
[47] M. Rosi, F. Iskandar, and M. Abdullah, "Synthesis of Carbon Nanopores with Varying Amounts of NaOH and Their Application as Supercapacitors Synthesis of Carbon Nanopores with Varying Amounts of NaOH and Their Application as Supercapacitors," *Semin. Nas. Fis. Inst. Technol. Bandung*, pp. 74-77, 2013.
[48] T. S. Sinaga, "Manufacturing process and introduction of activated charcoal," pp. 1-9, 2003.
[49] L. Maulinda, Z. Nasrul, and D. N. Sari, "Journal of Unimal Chemical Technology Utilization of Cassava Peel as Raw Material for Activated Carbon," *J. Teknol. Kim. Unimal*, vol. 4, no. 2, pp. 11-19, 2015.
[50] L. A. Didik, "Determination Of Crystal Buzz Size Of Cucr0.98ni0.02o2 By Using X-Ray Difraction (Xrd) And Scanning Electron Microscope (Sem)," *Indones. Phys. Rev.*, vol. 3, no. 1, pp. 6-14, 2020, doi: 10.29303/ipr.v3i1.37.
[51] P. Elizabeth and S. Africa, "Asian Journal of Phytomedicine," vol. 2, no. 1, pp. 11-21, 2014.
[52] W. Lu and D. D. L. Chung, "Preparation of conductive carbons with high surface area," *Carbon N. Y.*, vol. 39, no. 1, pp. 39-44, 2001, doi: 10.1016/S0008-6223(00)00077-4.